JOURNAL OF COMPUTATIONAL PHYSICS 16, 360–370 (1974)

Numerical Calculation of Nonunique Solutions of a Two-Dimensional Sinh-Poisson Equation

B. E. McDONALD

Naval Research Laboratory, Washington, D. C. 20375

Received May 22, 1974; revised September 4, 1974

We give a method for computing nontrivial solutions to the nonlinear partial differential equation $\nabla^2\Psi + \lambda^2 \sinh \Psi = 0$, with $\Psi = 0$ on a square boundary. The method consists of a Newton–Raphson iteration, in which successive corrections to Ψ must satisfy a linearized partial differential equation. We give a direct solution algorithm for the linearized equation, which is suitable for small meshes. Using this method, we establish the nonuniqueness of solutions by finding six solutions for the same value of λ. Calculation of these solutions required from 4 to about 40 iterations each, depending upon the accuracy of the initial approximation. These solutions are the lowest-mode members of three classes of solutions possessing (1) rectangular, (2) quasicylindrical, and (3) diagonal symmetry.

I. INTRODUCTION

Statistical mechanical considerations applied to equilibrium states of a two-dimensional guiding center plasma [1] lead to the following equation for the electrostatic potential $\phi(X, Y)$ inside a long waveguide.

$$((\partial^2/\partial X^2) + (\partial^2/\partial Y^2))\,\phi = -4\pi e[n_+ e^{-\beta e\phi} - n_- e^{\beta e\phi}], \tag{1}$$

where e (>0) is the absolute value of the electronic charge, β is a negative [1] constant playing the role of the familiar $1/kT$ of statistical mechanics, and n_+ and n_- are constant number densities of positive and negative charges at the boundaries, where ϕ is taken to be zero.

The coordinates X and Y define a plane cutting across the waveguide. There is assumed to be no dependence on the coordinate Z (along the length of the waveguide).

A set of physically interesting solutions arise [2] when we take

$$n_+ = n_- = n, \tag{2}$$

and look for solutions inside a square of side L. In this case, we can put (1) into the dimensionless form

$$\nabla^2\Psi + \lambda^2 \sinh \Psi = 0, \tag{3}$$

where

$$\Psi = e\beta\phi, \tag{4}$$

$$\lambda^2 = -8\pi e^2 n\beta L^2, \tag{5}$$

and

$$\nabla^2 = (\partial^2/\partial x^2) + (\partial^2/\partial y^2), \tag{6}$$

with the new dimensionless coordinates $x = X/L$ and $y = Y/L$. The boundary conditions accompanying (3) are

$$\Psi = 0 \tag{7}$$

on the boundary of the square $0 \leqslant x \leqslant 1, 0 \leqslant y \leqslant 1$.

Equation (3) is nonlinear, and is not subject to the usual uniqueness theorems which arise from the investigation of linear equations. In fact we have thus far found (and shall describe below) six different types of solutions for the same value of λ. These multiple solutions describe equilibrium states with the same physical parameters, including size and temperature. The physical implications of these states will be discussed elsewhere [3].

Equations (3) and (7) are satisfied trivially by $\Psi(x, y) = 0$. Attempts to find nontrivial solutions by the methods of Marder and Weitzner [4] or by straightforward laplacian operator inversion have been unsuccessful [5, 6]. In order to find the nontrivial solutions, we shall construct an iterative method which specifically excludes the solution $\Psi = 0$.

Let us begin with a trial solution $W(x, y)$. We define a residual function

$$R(x, y) = (\nabla^2 W + \lambda^2 \sinh W)/(W, W), \tag{8}$$

where the inner product (A, B) of two real functions A and B is defined by

$$(A, B) = \int_0^1 dx \int_0^1 dy\, A(x, y)\, B(x, y). \tag{9}$$

Thus R tends to zero as W approaches a nontrivial solution, but diverges if W tends to zero everywhere.

If we introduce a small variation $\delta W(x, y)$ in W, the resulting linear change in R is

$$\delta R(x, y) = (\nabla^2 \delta W + \lambda^2 \delta W \cosh W - 2(\delta W, W) R)/(W, W). \tag{10}$$

We attempt to bring R to zero in the sense of a Newton–Raphson iteration, i.e., by setting $\delta R = -R$. The variation δW must then satisfy the integro-differential equation

$$\nabla^2 \delta W + \lambda^2 \delta W \cosh W - 2(\delta W, W) R = -(W, W) R. \tag{11}$$

In terms of a function v which satisfies

$$\nabla^2 v + \lambda^2 v \cosh W = (W, W) R, \tag{12}$$

subject to $v = 0$ on the boundary, the solution to (11) is

$$\delta W(x, y) = v(x, y)/[2(v, W)/(W, W) - 1]. \tag{13}$$

Having found δW, we correct the trial solution:

$$W \to W + \delta W. \tag{14}$$

Nontrivial solutions to (3) have been found using the iteration loop consisting of the operations called for in Eqs. (8), (12), (13), and (14) carried out in cyclical order. The initial approximation $W(x, y)$ must be chosen judiciously with some thought given to the probable form of the particular solution $\Psi(x, y)$ being sought. Most of the solutions generated thus far began with products of sine waves in the x and y directions with some suitably chosen amplitude. Before describing the types of solutions found, we shall outline the method used to solve the linearized Eq. (12).

II. Direct Solution of the Linearized Equation

The iteration loop (3)–(14) calls for the solution of the linear partial differential Eq. (12) once per iteration cycle. The choice of a numerical solution method for (12) should take into account the following two points. (1) The right-hand side of (12) changes significantly in magnitude and spatial form each time the cycle (8)–(14) is executed, so that no accurate first approximation for v is available; and (2) the finite difference representation of the operator on the left-hand side of (12) (see (15) below) is a matrix which is nondiagonally dominant and is neither positive or negative definite. The first point suggests that iterative methods in general are at a disadvantage in that each pass through Eqs. (8)–(14) might require many subiterations for convergence of (12). The second point detracts from the usefulness of familiar successive over relaxation (SOR), alternating direction implicit (ADI), and variational methods [7]. Application of these methods in this case can result in convergence for some spectral components of the solution, but divergence for others.

Thus we are led to consider a direct solution method similar to one used by Roache [8] to solve Poisson's equation. The method is conceptually simple, but in practice roundoff error propagation restricts its use to small meshes. We can represent (12) on a discrete rectangular mesh (NX by NY) by a five-point difference equation of the form

$$[v(i+1,j) - 2v(i,j) + v(i-1,j)]/\delta x^2 + [v(i,j+1) - 2v(i,j) + v(i,j-1)]/\delta y^2 + q(i,j)\,v(i,j) = s(i,j), \tag{15}$$

for $2 \leqslant i \leqslant NX - 1$ and $2 \leqslant j \leqslant NY - 1$. The boundary condition is $v = 0$ on the boundaries, i.e., $v(1,j) = v(NX,j) = v(i,1) = v(i,NY) = 0$. If the solution were known on both rows $j = 1$ and $j = 2$, one could in principle find it everywhere. This would be accomplished by a forward sweep in which one solves (15) for $v(i,j+1)$ in terms of values on rows j and $j-1$. This sweep would continue row-by-row until the entire mesh has been supplied with known values of v.

The boundary condition sets $v = 0$ on row $j = 1$, and at the end points (1, 2) and (NX, 2) of row $j = 2$. Thus before beginning the forward sweep we must determine $NX - 2$ unknown v values on row $j = 2$. To find these we calculate a set of "basis functions" v_k, linearly independent solutions to (15) satisfying $v_k = 0$ on the three boundaries $i = 1$, $j = 1$, and $i = NX$. These solutions are swept forward after definition on rows $j = 1$ and 2, and nonzero values result on row $j = NY$. We then form a linear combination of the v_k which satisfies the boundary condition on the fourth boundary $j = NY$, and is the desired solution to (15).

We first define v_1 from

$$\begin{aligned} v_1(i,1) &= 0, \\ v_1(i,2) &= 0, \end{aligned} \tag{16}$$

sweeping the solution across the mesh using (15). Then we calculate the other v_k, $2 \leqslant k \leqslant NX - 1$, from

$$\begin{aligned} v_k(i,1) &= 0, \\ v_k(i,2) &= \delta_{ik}, \end{aligned} \tag{17}$$

where $\delta_{ik} = 1$ for $i = k$, and is zero otherwise. The solutions initiated by (17) are swept forward with $s = 0$, i.e., the homogeneous form of Eq. (15).

The desired solution to (15) is the linear combination

$$v(i,j) = v_1(i,j) + \sum_{k=2}^{NX-1} c_k v_k(i,j), \tag{18}$$

which is zero on row $j = NY$. Thus the coefficients c_k are determined from the following set of linear equations.

$$\sum_{k=2}^{NX-1} c_k v_k(i, NY) = -v_1(i, NY), \tag{19}$$

$2 \leqslant i \leqslant NX - 1$. Since only the row $j = NY$ is used in determining c_k, only this row is retained from each of the v_k in order to conserve core storage. Once the c_k are known, we calculate $v(i, j)$ by a forward sweep initiated by

$$\begin{aligned} v(i, 1) &= 0, \\ v(i, 2) &= c_i, \qquad 2 \leqslant i \leqslant NX - 1. \end{aligned} \tag{20}$$

The propagation of roundoff errors during a forward sweep is best described by considering Poisson's equation with $\delta x = \delta y$. A more complete description is given by Roache [8]. As random errors are introduced, an exponentially increasing spurious solution $\tilde{v}$ is initiated which corresponds to the fastest growing solution of $\nabla^2 \tilde{v} = 0$ which the discrete grid can mimic. This solution changes sign from grid point to grid point in both directions, with constant amplitude in x and exponentially increasing amplitude in y. The continuous analog for this solution is $\tilde{v} \propto \sin kx \exp ky$. One can show readily that the amplitude of this spurious solution increases by a factor of $3 + 2\sqrt{2} \approx 5.83$ from row-to-row in the y direction. Thus an initial roundoff error of 10^{-16} increases to 10^{-5} after having been propagated 14 rows forward. This limits the application of the method to small meshes, but even so, valuable information about the solutions of (3) has been gained through its use. Most of the solutions found thus far possess some kind of symmetry which allows (3) to be solved in a quadrant of the unit square, effectively increasing the resolution by a factor of 2.

III. Discussion of the Solutions

Figures 1–6 show six different types of solutions of (3) obtained for $\lambda^2 = 19$. The behavior of the solutions as a function of λ^2 and their physical implications will be discussed in a future paper [3]. The existence of these different solutions for the same boundary conditions and value of λ^2 establishes that (3) does not possess a unique solution. This nonuniqueness was suggested by Fisher [5], after investigation [4, 9] of an equation similar to (3), but with the hyperbolic sine replaced by exp.

The six solutions shown below were calculated on a 15×15 grid. The first four possess rectangular symmetry, and were calculated in one quadrant only by a

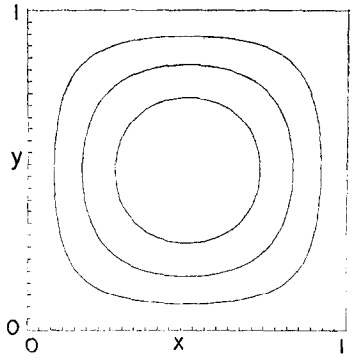

FIG. 1. Contours of constant Ψ for $\lambda^2 = 19$. Maximum and minimum values of Ψ are $\Psi_{\max} = 0.630$, $\Psi_{\min} = 0$. Contour spacing for Figs. 1–5 is 0.25 $\Psi_{\max}$. Tick marks on the border are grid-point locations. Solid contours are positive, dashed contours are negative, and dot–dash contours are zero.

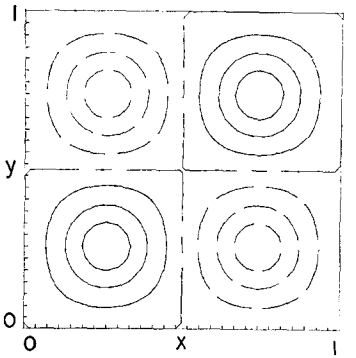

FIG. 2. $\lambda^2 = 19$, $\Psi_{\max} = 4.781$, $\Psi_{\min} = -4.781$.

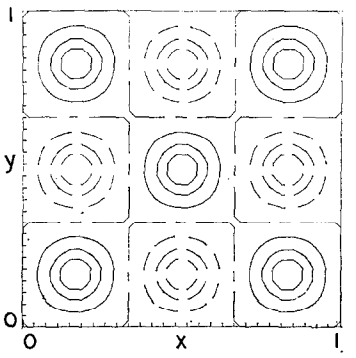

FIG. 3. $\lambda^2 = 19$, $\Psi_{\max} = 5.657$, $\Psi_{\min} = -5.657$.

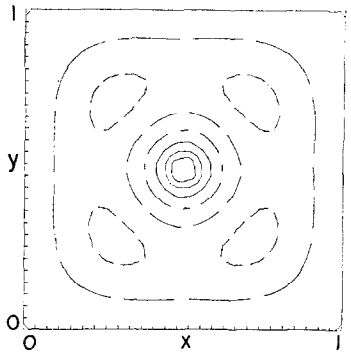

FIG. 4. $\lambda^2 = 19$, $\Psi_{max} = 6.123$, $\Psi_{min} = -3.478$.

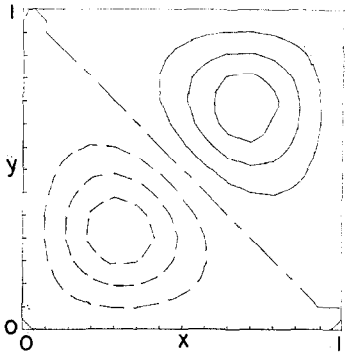

FIG. 5. $\lambda^2 = 19$, $\Psi_{max} = 3.666$, $\Psi_{min} = -3.666$.

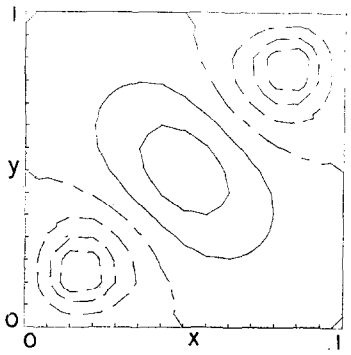

FIG. 6. $\lambda^2 = 19$, $\Psi_{max} = 3.513$, $\Psi_{min} = -4.888$. Contour spacing is $0.25 \mid \Psi_{min} \mid$.

simple variation of the method given above. These solutions are probably adequately resolved, since they vary smoothly over the unit square, which is covered by an effective 28×28 grid. The last two solutions have been computed by the above method without change, with an overall resolution of 15×15 points. Despite the lower resolution, they do point out an interesting alternative to the class of solutions represented in Figs. 1–3.

As an indication of the accuracy to which (3) has been solved for each of the cases, we define

$$f(i,j) = \Delta^2\Psi(i,j) + \lambda^2 \sinh \Psi(i,j), \tag{21}$$

$$g(i,j) = |\Delta^2\Psi(i,j)| + |\lambda^2 \sinh \Psi(i,j)|, \tag{22}$$

where Δ^2 is the finite difference operator used in (15). We then define a root-mean-square error,

$$\epsilon = \left(\sum f^2 \Big/ \sum g^2\right)^{1/2}, \tag{23}$$

where the summation is over the interior mesh, $2 \leqslant i \leqslant 14$, $2 \leqslant j \leqslant 14$. The RMS errors for the solutions in Figs. 1–6 are, repectively, 1.70, 1.97, 0.83, 1.18, 4.71, and 0.56 times 10^{-6}.

Thus the finite difference equations have been solved quite accurately. However, these figures do not in themselves reveal the closeness of the discrete solutions given here to their continuous analogs. We can obtain a measure of the discreteness error by comparing results from two different expressions for the electrostatic energy. Let us define

$$\mathscr{E}_1 = \int_0^1 dx \int_0^1 dy\, (\nabla\Psi)^2, \tag{24}$$

$$\mathscr{E}_2 = -\int_0^1 dx \int_0^1 dy\, \Psi \nabla^2\Psi. \tag{25}$$

In the continuum limit, the boundary condition (7) results in $\mathscr{E}_1$ and $\mathscr{E}_2$ being equal. For the discrete solutions, the following second-order accurate expressions were used as approximations to $\mathscr{E}_1$ and $\mathscr{E}_2$.

$$E_1 = \tfrac{1}{2} \sum_{i=1}^{I-1} \sum_{j=1}^{J-1} (\Psi(i+1,j+1) - \Psi(i,j))^2 + (\Psi(i,j+1) - \Psi(i+1,j))^2, \tag{26}$$

$$E_2 = -\sum_{i=2}^{I-1} \sum_{j=2}^{J-1} \Psi(i,j)[\Psi(i+1,j) + \Psi(i-1,j) + \Psi(i,j+1) + \Psi(i,j-1) - 4\Psi(i,j)]. \tag{27}$$

Here I and J are the total numbers of mesh points in the x and y directions, allowing for folding into four quadrants in the cases of Figs. 1–4. For the six solutions given here, I and J are equal, and are 28 for Figs. 1–4, and 15 for Figs. 5 and 6. The different summation limits in (26) and (27) are due to cell-centered differencing in in (26) as opposed to grid point-centered differencing in (27). Values for E_1 and E_2 and their relative difference, $2 \mid E_1 - E_2 \mid /(E_1 + E_2)$, are given in Table I. One notices that the relative differences are in the range 0.2–7 %, and that the greater differences belong to the more crudely resolved solutions Thus we take these relative differences as indicators of the magnitude of the truncation error for each of the cases.

TABLE I

Electrostatic Energies Calculated Independently from (26) and (27) for Figs. 1–6

	E_1	E_2	Relative difference
1	4.88	4.89	.002
2	13.20	13.42	.017
3	29.18	30.58	.047
4	9.22	9.49	.029
5	7.01	7.18	.024
6	9.18	9.85	.070

The solutions in Figs. 1–3 are the first of a series of solutions generated by scale changes and folding. We find the Nth solution in the series by solving the transformed problem

$$\nabla'^2 \Psi + \lambda^2/N^2 \sinh \Psi = 0, \tag{28}$$

with $x' = N \cdot x$ and $y' = N \cdot y$, subject to $\Psi = 0$ on the boundary of the square $0 \leqslant x' \leqslant 1$, $0 \leqslant y' \leqslant 1$. We calculate the lowest-mode solution to (28) (i.e., as in Fig. 1) and place N by N of these side-by-side in checkerboard fashion, with changes of sign from one to another. The result in xy space is a solution to (3) satisfying the proper boundary conditions. The checkerboard pattern satisfies (3) on the interior of each of the subsquares as a result of (28). On the boundaries of the subsquares, (3) is satisfied for the following reasons. Along one of the sides of a subsquare, Ψ is zero, and thus the second derivative in that direction is zero. In the transverse direction, a point of inflection results from the asymmetrical

folding, so that the second derivative in this direction is also zero. Thus (3) is satisfied everywhere within the "super square" $0 < x < 1$, $0 < y < 1$.

Another sequence of solutions is suggested by Figs. 1 and 4. One notices that the contours near the centers of Figs. 1 and 4 are approximately circular, but that angular dependence becomes more pronounced near the square boundaries. This suggests a comparison of these solutions with solutions of (3) in cylindrical coordinates with no angular dependence. Such solutions have been investigated recently by Fisher [5]. One finds these cylindrical solutions by solving the one-dimensional radial equation

$$(d^2/dr^2)\,\Psi + (1/r)(d\Psi/dr) + \lambda^2 \sinh \Psi = 0, \tag{29}$$

subject to continuity of Ψ at the origin, and $\Psi = 0$ at a suitable value of r. For a given λ, a sequence of solutions to (29) exists, with increasing numbers of radial oscillations and varying values of slope at the outer boundary. One finds that near the centers, the solutions of Figs. 1 and 4 bear a close resemblance to the two lowest-mode solutions of (29). These solutions might be thought of as the result of a continuous process beginning with a solution of (29) inside a circular boundary, followed by a gradual deformation of the boundary into a square, maintaining (3) all the while.

A third sequence of solutions is suggested by Figs. 1, 5, and 6, with the primary variation being along a diagonal of the square. To date we have found one higher-mode solution than the one in Fig. 6, although the current limitation to small meshes results in rather poor resolution. This solution has a zero diagonal as does Fig. 5, and has three nodes along the other diagonal. Other types of solutions no doubt exist, the most obvious being a class of solutions with rectangular symmetry, having different numbers of nodes in the x and y directions.

ACKNOWLEDGMENT

I would like to thank Drs. D. L. Book and S. Fisher for their helpful discussions during the preparation of this work.

Support was furnished by the Office of Naval Research.

REFERENCES

1. GLENN JOYCE AND DAVID MONTGOMERY, *J. Plasma Phys.* **10** (1973), 107–121.
2. GLENN JOYCE AND DAVID MONTGOMERY, *Phys. Fluids* **17** (1974), 1139–1145.
3. S. FISHER, D. L. BOOK, AND B. E. MCDONALD, to be published.
4. B. MARDER AND H. WEITZNER, *J. Plasma Phys.* **12** (1970), 435–445.
5. S. FISHER, personal communication.
6. GLENN JOYCE, personal communication to D. L. Book.

7. RICHARD S. VARGA, "Matrix Iterative Analysis," Chaps. 6–7, Prentice–Hall, Englewood Cliffs, NJ, 1962.
8. PATRICK J. ROACHE, "Computational Fluid Dynamics," Pp. 124–131, Hermosa Publishers, Albuquerque, NM, 1972.
9. S. FISHER, *Phys. Fluids* **14** (1971), 962–966.